

Topological susceptibility in two flavors lattice QCD with exact chiral symmetry

Ting-Wai Chiu^{1,2,3}, Tung-Han Hsieh^{*4}, Yao-Yuan Mao¹ (TWQCD Collaboration)

¹ Physics Department, National Taiwan University, Taipei 10617, Taiwan

² Center for Quantum Science and Engineering, National Taiwan University, Taipei 10617, Taiwan

³ Center for Theoretical Sciences, National Taiwan University, Taipei 10617, Taiwan

⁴ Research Center for Applied Sciences, Academia Sinica, Taipei 115, Taiwan

We determine the topological susceptibility of the gauge configurations generated by lattice simulations using 2 flavors of optimal domain-wall fermion on the $16^3 \times 32$ lattice with length 16 in the fifth dimension, at the inverse lattice spacing $a^{-1} \simeq 1.9$ GeV. Using the adaptive thick-restart Lanczos algorithm, we project the low-lying eigenmodes of the overlap Dirac operator, and obtain the topological charge Q_t of each gauge configuration in eight ensembles with pion masses in the range 230 – 580 MeV. From our result of Q_t , we compute the topological susceptibility and the second normalized cumulant. Our result of the topological susceptibility agrees with the sea-quark mass dependence predicted by the next-to-leading order chiral perturbation theory, and provides a determination of both the chiral condensate and the pion decay constant.

*The XXIX International Symposium on Lattice Field Theory - Lattice 2011
July 10-16, 2011
Squaw Valley, Lake Tahoe, California*

*Speaker.

1. Introduction

The vacuum of Quantum Chromodynamics (QCD) has a non-trivial topological structure. The cluster property and the gauge invariance require that the ground state must be the θ vacuum, a superposition of gauge configurations in different topological sectors. The topological susceptibility (χ_t) is the most crucial quantity to measure the topological fluctuations of the QCD vacuum, which plays an important role in breaking the $U_A(1)$ symmetry. Theoretically, χ_t is defined as

$$\chi_t = \int d^4x \langle \rho(x) \rho(0) \rangle, \quad \rho(x) = \frac{1}{32\pi^2} \varepsilon_{\mu\nu\lambda\sigma} \text{tr}[F_{\mu\nu}(x) F_{\lambda\sigma}(x)], \quad (1.1)$$

where $\rho(x)$ is the topological charge density expressed in term of the matrix-valued field tensor $F_{\mu\nu}$. With mild assumptions, Witten [1] and Veneziano [2] obtained a relationship between the topological susceptibility in the quenched approximation and the mass of η' meson (flavor singlet) in the full QCD. This implies that the mass of η' is essentially due to the axial anomaly relating to non-trivial topological fluctuations, unlike those of the (non-singlet) approximate Goldstone bosons.

From (1.1), we obtain

$$\chi_t = \frac{\langle Q_t^2 \rangle}{\Omega}, \quad Q_t \equiv \int d^4x \rho(x), \quad (1.2)$$

where Ω is the volume of the system, and Q_t is the topological charge (which is an integer for QCD). Thus, one can determine χ_t by counting the number of gauge configurations for each topological sector. Furthermore, we can also obtain the second normalized cumulant

$$c_4 = -\frac{1}{\Omega} [\langle Q_t^4 \rangle - 3\langle Q_t^2 \rangle^2], \quad (1.3)$$

which is related to the leading anomalous contribution to the $\eta' - \eta'$ scattering amplitude in QCD, as well as the dependence of the vacuum energy on the vacuum angle θ .

However, for lattice QCD, it is difficult to extract $\rho(x)$ and Q_t unambiguously from the gauge link variables, due to their rather strong fluctuations. To circumvent this difficulty, we may consider the Atiyah-Singer index theorem [3], $Q_t = n_+ - n_- = \text{index}(\mathcal{D})$, where n_{\pm} is the number of zero modes of the massless Dirac operator $\mathcal{D} \equiv \gamma_{\mu}(\partial_{\mu} + igA_{\mu})$ with \pm chirality.

For lattice QCD with exact chiral symmetry, it is well-known that the overlap Dirac operator [4, 5] in a topologically non-trivial gauge background possesses exact zero modes (with definite chirality) satisfying the Atiyah-Singer index theorem. Thus we can obtain the topological charge from the index of the overlap Dirac operator. Writing the overlap Dirac operator as

$$D_o = m_0 \left(1 + \gamma_5 \frac{H_w}{\sqrt{H_w^2}} \right),$$

where H_w is the standard Hermitian Wilson operator with negative mass $-m_0$ ($0 < m_0 < 2$), then its index is

$$\text{index}(D) = \text{Tr} \left[\gamma_5 \left(1 - \frac{D_o}{2m_0} \right) \right] = n_+ - n_- = Q_t,$$

where Tr denotes trace over Dirac, color, and site indices.

In Ref [6], we measure the topological charge of the gauge configurations generated by lattice simulations of two flavors QCD on a $16^3 \times 32$ lattice, with the optimal domain-wall fermion (ODWF) [7] at $N_s = 16$, and plaquette gauge action at $\beta = 5.95$, for eight sea-quark masses $m_q a = 0.01, \dots, 0.08$ with the interval 0.01.

Mathematically, ODWF is a theoretical framework which can preserve the chiral symmetry optimally for any given N_s , with a set of analytical weights $\{\omega_s, s = 1, \dots, N_s\}$, one for each layer in the fifth dimension [7]. Thus the artifacts due to the chiral symmetry breaking with finite N_s can be reduced to the minimum, especially in the chiral regime. The 4-dimensional effective Dirac operator of massless ODWF is

$$D = m_0[1 + \gamma_5 S_{opt}(H_w)], \quad S_{opt}(H_w) = \frac{1 - \prod_{s=1}^{N_s} T_s}{1 + \prod_{s=1}^{N_s} T_s}, \quad T_s = \frac{1 - \omega_s H_w}{1 + \omega_s H_w}, \quad (1.4)$$

which is exactly equal to the Zolotarev optimal rational approximation of the overlap Dirac operator. That is, $S_{opt}(H_w) = H_w R_Z(H_w)$, where $R_Z(H_w)$ is the optimal rational approximation of $(H_w^2)^{-1/2}$ [8, 9].

We use the adaptive thick-restart Lanczos algorithm [10] to project the low-lying eigenmodes of the 4-dimensional effective Dirac operator (1.4), and obtain the topological charge Q_t of each gauge configuration. Then we compute the topological susceptibility χ_t and the second normalized cumulant c_4 , and compare our results to the Chiral Perturbation Theory (ChPT). We summarize the ChPT formulas as follows.

In 1992, Leutwyler and Smilga [11] derived the relationship between χ_t and the quark mass, at the leading order in ChPT. For 2 flavors QCD, it reads

$$\chi_t = \Sigma (m_u^{-1} + m_d^{-1})^{-1}, \quad (1.5)$$

where m_u, m_d are the quark masses, and Σ is the chiral condensate. This implies that in the chiral limit ($m_u \rightarrow 0$) the topological susceptibility is suppressed by the internal quark loops. Most importantly, (1.5) provides a viable way to extract Σ from χ_t in the chiral regime.

Recently, the topological susceptibility has been derived to the one-loop order in ChPT for an arbitrary number of flavors [12]. For $N_f = 2$ with degenerate u and d quark masses ($m_u = m_d \equiv m_q$), the formula reduces to

$$\frac{\chi_t}{m_q} = \frac{\Sigma}{2} \left\{ 1 - 3 \left(\frac{\Sigma m_q}{16\pi^2 F_\pi^4} \right) \ln \left(\frac{2\Sigma m_q}{F_\pi^2 \mu_{sub}^2} \right) + 32 \left(\frac{\Sigma}{F_\pi^4} \right) (2L_6 + 2L_7 + L_8) m_q \right\}, \quad (1.6)$$

where L_i are renormalized low-energy coupling constants defined at μ_{sub} [13]. In this work, we fix $\mu_{sub} = 770$ MeV.

In this proceeding, we review our result of topological susceptibility presented in Ref. [6].

2. Lattice Setup

Simulations are carried out for two flavors QCD on a $16^3 \times 32$ lattice at the lattice spacing $a \sim 0.1$ fm, for eight sea-quark masses $m_q a = 0.01, 0.02, 0.03, 0.04, 0.05, 0.06, 0.07$, and 0.08, respectively. For the quark part, we use the optimal domain-wall fermion with $N_s = 16$. For the

gluon part, we use the plaquette action at $\beta = 5.95$. An outline of our simulation algorithm and its acceleration with Nvidia GPUs have been presented in Refs. [14, 15].

For each sea-quark mass, we perform hybrid Monte-Carlo simulations on 30 GPUs independently, with each GPU generating 400 trajectories. After discarding 300 trajectories for thermalization, each GPU yields 100 trajectories. Thus, with 30 GPUs running independently, we accumulated total 3000 trajectories for each sea-quark mass. From the saturation of the binning error of the plaquette, as well as the evolution of the topological charge, we estimate the autocorrelation time to be around 10 trajectories. Thus we sample one configuration every 10 trajectories, then we have 300 configurations for each sea-quark mass. With a GPU cluster of 250 GPUs, we can simulate 8 sea-quark masses concurrently. It takes about 5 months to complete the simulations for the $\beta = 5.95$ ensemble.

We determine the lattice spacing by heavy quark potential with Sommer parameter $r_0 = 0.49$ fm. Using the linear fit, we obtain the lattice spacing in the chiral limit, $a = 0.1032(2)$ fm, which gives $a^{-1} = 1.911(4)(6)$ GeV, where the systematic error is estimated with the uncertainty of r_0 .

For each configuration, we calculate the zero modes plus 80 conjugate pairs of the lowest-lying eigenmodes of the overlap Dirac operator. We outline our procedures as follows. First, we project 240 low-lying eigenmodes of H_w^2 using adaptive thick-restart Lanczos algorithm (a -TRLan) [10], where each eigenmode has a residual less than 10^{-12} . Then we approximate the sign function of the overlap operator by the Zolotarev optimal rational approximation with 64 poles, where the coefficients are fixed with $\lambda_{max}^2 = (6.4)^2$, and λ_{min}^2 equal to the maximum of the 240 projected eigenvalues of H_w^2 . Then the sign function error is less than 10^{-14} . Using the 240 low-modes of H_w^2 and the Zolotarev approximation with 64 poles, we use the a -TRLan algorithm again to project the zero modes plus 80 conjugate pairs of the lowest-lying eigenmodes of the overlap operator, where each eigenmode has a residual less than 10^{-12} . We store all projected eigenmodes for the later use. In this work, we use the index of the zero modes to compute χ_t and c_4 .

3. Results

In Fig. 1, we plot the histogram of topological charge distribution for $m_q a = 0.01, 0.02, \dots, 0.08$ respectively. Evidently, the probability distribution of Q_t for each sea-quark mass behaves like a Gaussian, and it becomes more sharply peaked around $Q_t = 0$ as the sea-quark mass m_q gets smaller.

Using the result of Q_t , we compute the topological susceptibility χ_t (1.2), and the second normalized cumulant c_4 (1.3). In Table 1, we list our results of χ_t , c_4 , and the ratio c_4/χ_t . The error is estimated using the jackknife method with bin size of 10 configurations, with which the statistical error saturates.

Evidently, the statistical error of the topological susceptibility is about 10%, while that of c_4 is very large due to low statistics. Therefore, we cannot draw any conclusions from our result of c_4 , as well as from the ratio c_4/χ_t .

In Fig. 2-(a), we plot our data of χ_t versus the sea quark mass m_q . The data points of χ_t are well fitted by the Leutwyler and Smilga formula (1.5) with $\Sigma a^3 = 0.00200(15)$. The fitted curve is plotted as the solid line in Fig. 2-(a).

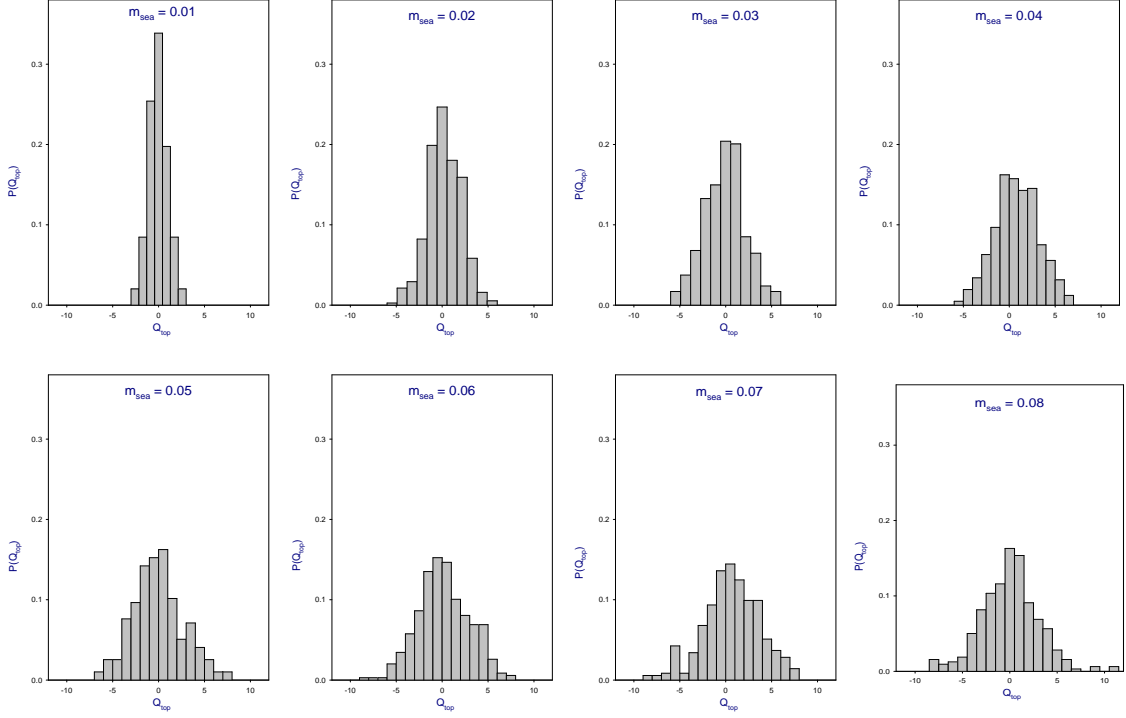


Figure 1: Histogram of topological charge distribution for eight sea quark masses, $m_q a = 0.01, 0.02, 0.03, 0.04, 0.05, 0.06, 0.07,$ and 0.08 respectively.

In Fig. 2-(b), we plot our data of χ_t/m_q versus the sea-quark mass m_q . The data points of χ_t/m_q are well fitted by the NLO ChPT formula (1.6) with $\Sigma a^3 = 0.0020(2)$, $F_\pi a = 0.048(7)$, and $(2L_6 + 2L_7 + L_8) = -0.0001(3)$, where $\mu_{sub} = 770$ MeV. Using $a^{-1} = 1.911(4)(6)$ GeV, we obtain $\Sigma = [241(6)(1) \text{ MeV}]^3$, and

$$F_\pi = 92(12)(2) \text{ MeV}, \quad (3.1)$$

where the errors represent a combined statistical error and the systematic error respectively.

In order to convert Σ to that in the $\overline{\text{MS}}$ scheme, we calculate the renormalization factor $Z_s^{\overline{\text{MS}}}(2 \text{ GeV})$ using the non-perturbative renormalization technique through the RI/MOM scheme [16], and our result is [17]

$$Z_s^{\overline{\text{MS}}}(2 \text{ GeV}) = 1.244(18)(39).$$

Then the value of Σ is transcribed to

$$\Sigma^{\overline{\text{MS}}}(2 \text{ GeV}) = [259(6)(7) \text{ MeV}]^3, \quad (3.2)$$

where the errors represent a combined statistical error (a^{-1} and $Z_s^{\overline{\text{MS}}}$) and the systematic error respectively. Since the present calculation is done at a single lattice spacing, the discretization error cannot be quantified reliably, but we do not expect much larger error because the optimal domain-wall fermion action is free from $O(a)$ discretization effects. Our result of Σ (3.2) is in good

$m_q a$	χ_t	c_4	c_4/χ_t
0.01	$1.13(10) \times 10^{-5}$	$-1.22(1.15) \times 10^{-5}$	$-1.07(1.01)$
0.02	$2.24(18) \times 10^{-5}$	$-3.79(2.77) \times 10^{-5}$	$-1.69(1.24)$
0.03	$3.29(27) \times 10^{-5}$	$-1.25(2.87) \times 10^{-5}$	$-0.04(0.87)$
0.04	$4.40(30) \times 10^{-5}$	$6.39(4.16) \times 10^{-5}$	$1.45(95)$
0.05	$5.31(41) \times 10^{-5}$	$5.75(7.96) \times 10^{-5}$	$1.08(1.50)$
0.06	$6.04(44) \times 10^{-5}$	$1.00(1.09) \times 10^{-4}$	$1.66(1.81)$
0.07	$7.24(55) \times 10^{-5}$	$-5.12(134) \times 10^{-6}$	$-0.07(1.86)$
0.08	$7.01(79) \times 10^{-5}$	$-7.10(6.58) \times 10^{-4}$	$-10.13(9.46)$

Table 1: The topological susceptibility χ_t , the second normalized cumulant c_4 , and their ratio c_4/χ_t , versus the sea quark masses, for $N_f = 2$ lattice QCD with the optimal domain-wall fermion.

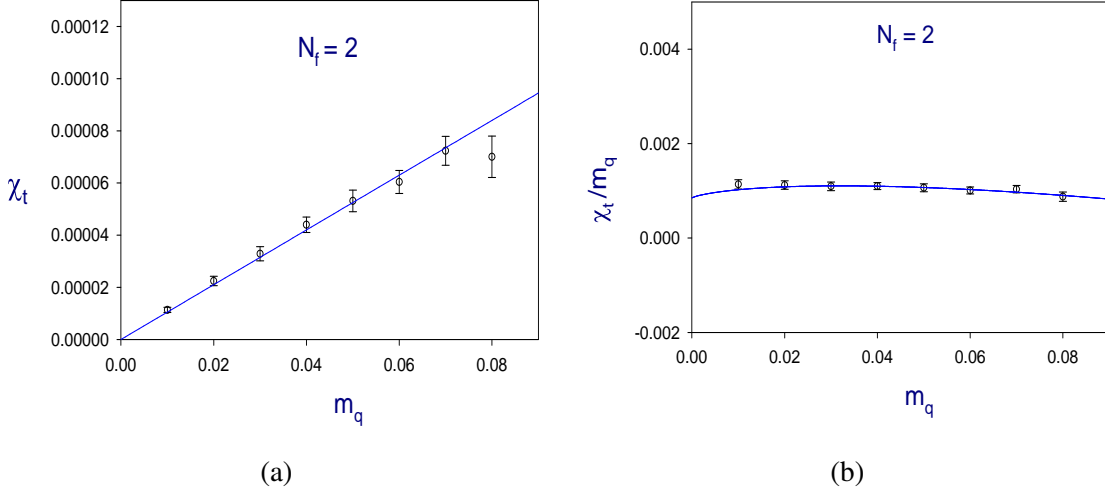


Figure 2: (a) The topological susceptibility χ_t , and (b) the ratio χ_t/m_q , versus the sea-quark mass m_q , for 2 flavors lattice QCD with ODWF.

agreement with that extracted from χ_t in (2+1) flavors QCD with domain-wall fermion [18], as well as with those extracted from χ_t in $N_f = 2$ and $N_f = 2 + 1$ lattice QCD with overlap fermion in a fixed topology [19, 20].

4. Concluding remark

To summarize, we measure the topological charge of the gauge configurations generated by lattice simulations of 2 flavors QCD with the optimal domain-wall fermion at $N_s = 16$ and plaquette gauge action at $\beta = 5.95$, on a $16^3 \times 32$ lattice. We use the adaptive thick-restart Lanczos algorithm to compute the low-lying eigenmodes of the overlap Dirac operator, and obtain the topological charge of each gauge configuration, and from which we compute the topological susceptibility for 8 sea-quark masses, each of 300 configurations. Our result of the topological susceptibility agrees with the sea-quark mass dependence predicted by the NLO ChPT formula (1.6), and gives the first

determination of both the pion decay constant (3.1) and the chiral condensate (3.2) simultaneously from the topological susceptibility.

Recently, we have also computed the mass and decay constant of the pseudoscalar meson for the same set of gauge configurations [21]. Our data is in good agreement with the sea-quark mass dependence predicted by the next-to-leading order (NLO) ChPT, and provides a determination of the low-energy constants \bar{l}_3 and \bar{l}_4 , the pion decay constant, the chiral condensate, and the average up and down quark mass. In view of our results in Refs. [6, 21], we are confident that the nonperturbative chiral dynamics of the sea quarks are well under control in our HMC simulations. Moreover, this also implies that one can perform a large-scale simulation of unquenched lattice QCD with ODWF, which not only preserves the chiral symmetry to a high precision, but also samples all topological sectors ergodically.

This work is supported in part by the National Science Council (Nos. NSC99-2112-M-002-012-MY3, NSC99-2112-M-001-014-MY3) and NTU-CQSE (No. 10R80914-4). We also thank NCHC and NTU-CC for providing facilities to perform part of our calculations.

References

- [1] E. Witten, Nucl. Phys. B **156**, 269 (1979).
- [2] G. Veneziano, Nucl. Phys. B **159**, 213 (1979).
- [3] M. F. Atiyah and I. M. Singer, Annals Math. **87**, 484 (1968).
- [4] H. Neuberger, Phys. Lett. B **417**, 141 (1998)
- [5] R. Narayanan and H. Neuberger, Nucl. Phys. B **443**, 305 (1995)
- [6] T. W. Chiu, T. H. Hsieh and Y. Y. Mao [TWQCD Collaboration], Phys. Lett. B **702**, 131 (2011).
- [7] T. W. Chiu, Phys. Rev. Lett. **90**, 071601 (2003); Nucl. Phys. Proc. Suppl. **129**, 135 (2004)
- [8] N. I. Akhiezer, "Theory of approximation", Dover, New York, 1992.
- [9] T. W. Chiu, T. H. Hsieh, C. H. Huang and T. R. Huang, Phys. Rev. D **66**, 114502 (2002)
- [10] I. Yamazaki, Z. Bai, H. Simon, L.W. Wang, and K. Wu, ACM Transactions on Mathematical Software, Vol. 37, No. 3, Article 27 (2010).
- [11] H. Leutwyler and A. Smilga, Phys. Rev. D **46**, 5607 (1992).
- [12] Y. Y. Mao and T. W. Chiu [TWQCD Collaboration], Phys. Rev. D **80**, 034502 (2009)
- [13] J. Gasser and H. Leutwyler, Nucl. Phys. B **250**, 465 (1985).
- [14] T. W. Chiu *et al.* [TWQCD Collaboration], PoS **LATTICE2009**, 034 (2009)
- [15] T. W. Chiu *et al.* [TWQCD Collaboration], PoS **LATTICE2010**, 030 (2010).
- [16] G. Martinelli, C. Pittori, C. T. Sachrajda, M. Testa and A. Vladikas, Nucl. Phys. B **445**, 81 (1995)
- [17] T. W. Chiu *et al.* [TWQCD Collaboration], "Nonperturbative renormalization of bilinear operators in lattice QCD with the optimal domain-wall fermion", in preparation.
- [18] T. W. Chiu, T. H. Hsieh and P. K. Tseng [TWQCD Collaboration], Phys. Lett. B **671**, 135 (2009)
- [19] S. Aoki *et al.* [JLQCD and TWQCD Collaborations], Phys. Lett. B **665**, 294 (2008)
- [20] T. W. Chiu *et al.* [JLQCD and TWQCD Collaborations], PoS **LATTICE2008**, 072 (2008).
- [21] T. W. Chiu, T. H. Hsieh and Y. Y. Mao [TWQCD Collaboration], arXiv:1109.3675 [hep-lat].